Supplementary information

Metabolic signature of ethanol-induced hepatotoxicity in HepaRG cells by LC-MS-based untargeted metabolomics

Elias Iturrospe [1,2,*], Katyeny Manuela da Silva [1], Rani Robeyns [1], Maria van de Lavoir [1], Joost Boeckmans [2], Tamara Vanhaecke [2], Alexander L.N. van Nuijs [1], Adrian Covaci [1,*]

[1] University of Antwerp, Toxicological Centre, Universiteitsplein 1, 2610 Antwerp, Belgium

[2] Vrije Universiteit Brussel, Department of *In Vitro* Toxicology and Dermato-cosmetology, Laarbeeklaan 103, 1090 Jette, Belgium

*** - Corresponding authors**
Adrian Covaci. E-mail: adrian.covaci@uantwerpen.be
Elias Iturrospe. E-mail: elias.iturrospe@uantwerpen.be

TABLE OF CONTENTS

Supporting Information - Section 5. Data processing

Supporting Information - Section 6. Metabolic changes in the intracellular fraction of HepaRG cells

Supporting Information - Section 7. Metabolic changes in the extracellular fraction of HepaRG cells

Supporting Information - Section 8. Examples of MS/MS spectra

Section 1. Sample preparation of HepaRG cells

Differentiated HepaRG cells were seeded in collagen-coated Permanox 2-well Lab-Tek chamber slides, which were placed within Petri dishes, at a concentration of 1 x 10^6 cells per well (day 0). For seeding of the cells, Basal Hepatic Medium with HepaRG Thaw, Seed and General-Purpose Supplement was used. The cells were incubated at 37 °C, 5% CO_2 and saturated humidity using a Galaxy 170 S incubator. On day 1 of incubation, the medium was replaced by Basal Hepatic Medium with HepaRG Maintenance and Metabolism Supplement. On days 3 and 6, the medium was renewed.

On day 7, cells were exposed to 368 mM of ethanol (i.e., IC_{10}, n = 6), 36.8 mM of ethanol (i.e., 1/10 IC_{10}, n = 6) or no ethanol (i.e., negative control, n = 6) and cultivated for another 24 h.

For the 48 h exposure group, cells were exposed to 284 mM of ethanol (i.e., IC_{10}, n = 6), 28.4 mM of ethanol (i.e., 1/10 IC_{10}, n = 6) or no ethanol (i.e., negative control, n = 6) and cultivated for another 48 h with renewal of ethanol containing media after 24 h. Cells were exposed to ethanol-containing medium in one well, while phosphate-buffered saline (PBS) with the same concentration of ethanol was added to the second well. In addition, two extraction blanks, not containing cells, were obtained for each exposure group using the same conditions.

1.1. Sample preparation of intracellular HepaRG extracts

After ethanol exposure, media were collected (SI-2.2) and the chamber slides were washed twice using PBS (37 °C) before snap-freezing with liquid N_2. Quenching was performed using 300 µL of a solution, which consisted of 80% (v/v) MeOH and 20% (v/v) of 10 mM NH_4COOCH_3 at -80 °C. After 2 min, the cells were scraped and transferred to a vial for liquid-liquid extraction (LLE), which contained 500 µL of a polar mixture and 420 µL of an apolar mixture (at -20 °C). The polar mixture consisted out of 1 mM $(NH_4)_2EDTA$ and 0.5 mM ascorbic acid in 5 mM NH_4COOCH_3 with 0.1% (v/v) $HCOOCH_3$ (pH 4.2). The apolar mixture consisted of 1 mM butylated hydroxytoluene (BHT) in $CHCl_3$. Another 300 µL of the quenching solution was used for rinsing and was collected in the same LLE-vial. Internal standard mixture 1 contained 22 µg/mL lauric acid-12,12,12-D_3, cholic acid-2,2,4,4-D_4, glyceryl tri(palmitate-1-^{13}C), 18:1-D_7 lyso PE, octanoyl-L-carnitine-(N-methyl-D_3) and ceramide (d18:1/18:1(9Z)-$^{13}C_{18}$) in $CHCl_3$. Internal standard mixture 2 contained 14 µg/mL hippuric acid-(phenyl-$^{13}C_6$), L-lysine-$^{13}C_6$-$^{15}N_2$, leucine-5,5,5-D_3, glucose-$^{13}C_6$, caffeine-$^{13}C_3$ and L-phenylalanine-$^{13}C_9$-^{15}N in H_2O/MeOH (1/1, v/v). Aliquots of 20 µL of internal standard mixtures 1 and 2 were added to each LLE-vial. The extraction mixture was subsequently vortexed for 90 s, equilibrated for 10 min on ice, centrifuged at 2,200 g for 7 min at room temperature and again equilibrated for 10 min on ice. A volume of 900 µL of the polar fraction (upper phase) was transferred to an Eppendorf tube, without transferring solid particles from the protein disk. After vortexing for 20 s, 450 µL was transferred to a second Eppendorf tube after which the liquid of both Eppendorf tubes was evaporated using pure, dry nitrogen at room temperature. 240 µL of the apolar fraction (lower phase) was

transferred to a Reacti-Vial. After vortexing for 20 s, 120 µL was transferred to a second Reacti-Vial, after which the liquid was evaporated using pure, dry N_2 at room temperature. Dried extracts were stored at -80 °C and reconstituted directly before analysis. Each fraction (polar and apolar) was divided into two subfractions right before the evaporation step, in order to analyze each subfraction using a different polarity during liquid chromatography (LC) – (drift tube ion mobility (DTIM) – high resolution mass spectrometry (HRMS) acquisitions. Polar and apolar samples were reconstituted on ice using 60 µL of ACN/H_2O (65/35, v/v) and IPA/MeOH (35/65, v/v), respectively. After vortexing for 90 s, samples were filtered using 0.2 µm nylon centrifugal filters and centrifugated at 14,000 g for 2 min at room temperature. 10 µL of each sample was transferred to an LC-vial to create a QC pool. Another 20 µL of each sample was transferred to a Greiner Bio-One 384-well plate (small volume). Surrounding wells were filled with solvent blanks and the well plate was sealed using aluminum adhesive. Both the well plate and the QC pool were transferred to the autosampler (4 °C) right before analysis.

1.2. Sample preparation of extracellular HepaRG extracts

After exposure of HepaRG cells in Permanox 2-well Lab-Tek chamber slides, the incubation medium (1.2 mL per well) was extracted in separate Eppendorf tubes. Blank media (n = 4; 2 for each exposure group) were obtained after incubation without HepaRG cells and were treated identically to other samples. From the collected medium, 320 µL was transferred to a second Eppendorf tube, to which 725 µL of a -80 °C quenching solution was added. The quenching solution consisted out of 80% (v/v) MeOH and 20% (v/v) of 10 mM NH_4COOCH_3. After vortexing for 60 s, 980 µL of the quenched medium was transferred to an LLE-vial, which contained 500 µL of a polar mixture and 420 µL of an apolar mixture (-20 °C). The polar mixture consisted out of 1 mM $(NH_4)_2EDTA$ and 0.5 mM ascorbic acid in 5 mM NH_4COOCH_3 with 0.1% (v/v) $HCOOCH_3$ (pH 4.2). The apolar mixture consisted of 1 mM butylhydroxytoluene (BHT) in $CHCl_3$. Twenty µL of internal standard mixture 1 and 2 were added. Internal standard mixture 1 contained 18.2 µg/mL lauric acid-12,12,12-D_3, cholic acid-2,2,4,4-D_4, glyceryl tri(palmitate-1-^{13}C), 18:1-D_7 lyso PE, octanoyl-L-carnitine-(N-methyl-D_3) and ceramide (d18:1/18:1(9Z)-$^{13}C_{18}$) in $CHCl_3$. Internal standard mixture 2 contained 18 µg/mL hippuric acid-(phenyl-$^{13}C_6$), L-lysine-$^{13}C_6$-$^{15}N_2$, leucine-5,5,5-D_3, glucose-$^{13}C_6$, caffeine-$^{13}C_3$ and L-phenylalanine-$^{13}C_9$-^{15}N in H_2O/MeOH (1/1, v/v). The LLE vial was subsequently vortexed for 90 s, equilibrated for 10 min on ice, centrifuged at 2,200 g for 7 min at room temperature and again equilibrated for 10 min on ice. Thousand µL of the polar fraction (upper phase) was transferred to an Eppendorf tube, without transferring solid particles from the protein disk. After vortexing for 20 s, 500 µL was transferred to a second Eppendorf tube after which the liquid of both Eppendorf tubes was evaporated using pure, dry nitrogen at room temperature. 290 µL of the apolar fraction (lower phase) was transferred to a Reacti-Vial. After vortexing for 20 s, 145 µL was transferred to a second Reacti-Vial, after which the liquid was evaporated using pure, dry N_2 at room temperature. Dried extracts were stored at -80 °C and reconstituted directly before analysis. Each fraction (polar and apolar) was divided in two subfractions right

before the evaporation step, in order to analyze each subfraction using a different polarity during LC-(DTIM)-HRMS acquisitions. Polar and apolar samples were reconstituted on ice using 60 µL of ACN/H_2O (65/35, v/v) and IPA/MeOH (35/65, v/v), respectively. After vortexing for 90 s, samples were filtered using 0.2 µm nylon centrifugal filters and centrifugated at 14,000 g for 2 min at room temperature. 10 µL of each sample was transferred to an LC-vial to create a QC pool. Another 20 µL of each sample was transferred to a Greiner Bio-One 384-well plate (small volume). Surrounding wells were filled with solvent blanks and the well plate was sealed using aluminum adhesive. Both the well plate and the QC pool were transferred to the autosampler (4 °C) right before analysis.

1.3. Optimization of dilution factor for extracellular HepaRG extracts

The sample preparation of the extracellular fraction of HepaRG samples was based on the method of Cuykx *et al.*[1] and Dettmer *et al.*[2]. Because of the high dynamic range of metabolites, some metabolites are highly abundant and cause signal saturation during LC-MS analyses, which impairs mass accuracy and disables calculations of reliable fold changes between controls and exposed groups. Other metabolites are less abundant and cause low signal intensities or might be undetectable. In order to find a balance between the high and low abundant metabolites, the dilution factor used during sample preparation was optimized.[3]
During experiments for optimization of the dilution factor, the same sample preparation method was used as described in SI-1.2. The volume of cell medium, quenching solution and solutions used for LLE were multiplied by a factor of 3. After eight days of incubation of HepaRG cells (i.e., following the same procedure as described for the negative control group in SI-1), 960 µL of the medium was collected and 2175 µL of -80 °C quenching solution was added (80% (v/v) MeOH and 20% (v/v) of 10 mM NH_4COOCH_3). After vortexing for 60 s, 2940 µL of the quenched medium was transferred to an LLE-vial, which contained 1560 µL of a polar mixture and 1320 µL of an apolar mixture (-20 °C). The polar mixture consisted out of 1 mM $(NH_4)_2EDTA$ and 0.5 mM ascorbic acid in 5 mM NH_4COOCH_3 with 0.1% (v/v) $HCOOCH_3$ (pH 4.2). The apolar mixture consisted of 1 mM butylhydroxytoluene (BHT) in $CHCl_3$. The LLE vial was subsequently vortexed for 90 s, equilibrated for 10 min on ice, centrifuged at 2,200 g for 7 min at room temperature and again equilibrated for 10 min on ice. 3000 µL of the polar fraction (upper phase) was transferred to an Eppendorf tube, without transferring solid particles from the protein disk. After vortexing for 20 s, 1500 µL was transferred to a second Eppendorf tube after which the liquid of both Eppendorf tubes was evaporated using pure, dry nitrogen at room temperature. 870 µL of the apolar fraction (lower phase) was transferred to a Reacti-Vial. After vortexing for 20 s, 435 µL was transferred to a second Reacti-Vial, after which the liquid was evaporated using pure, dry N_2 at room temperature. Dried extracts were stored at -80 °C and reconstituted directly before analysis. Each fraction (polar and apolar) was divided into two subfractions right before the evaporation step, in order to analyze each subfraction using a different polarity during LC-HRMS acquisitions. Polar and apolar samples were reconstituted on ice using 60 µL of

ACN/H_2O (65/35, v/v) and IPA/MeOH (35/65, v/v), respectively. The polar reconstitution solvent contained 1 µg/mL of hippuric acid-(phenyl-$^{13}C_6$), L-lysine-$^{13}C_6$-$^{15}N_2$, leucine-5,5,5-D_3, glucose-$^{13}C_6$, caffeine-$^{13}C_3$ and L-phenylalanine-$^{13}C_9$-^{15}N. The apolar reconstitution solvent contained 1 µg/mL of lauric acid-12,12,12-D_3, cholic acid-2,2,4,4-D_4, glyceryl tri(palmitate-1-^{13}C), 18:1-D_7 lyso PE, octanoyl-L-carnitine-(N-methyl-D_3) and ceramide (d18:1/18:1(9Z)-$^{13}C_{18}$). After vortexing for 90 s, serial dilutions were made from the original sample (Fig. SI-1.3.1) using the abovementioned polar and apolar reconstitution solvents as dilution solvents. All samples were filtered using 0.2 µm nylon centrifugal filters and centrifugated at 14,000 g for 2 min at room temperature. 20 µL of each sample from the dilution experiment was transferred to a Greiner Bio-One 384-well plate (small volume). Surrounding wells were filled with solvent blanks and the well plate was sealed using aluminum adhesive. The 384-well plate was transferred to the autosampler (4 °C) right before analysis. Samples were ordered from low to high concentration for instrumental injection and data acquisition. Each sample was injected *in duplo*.

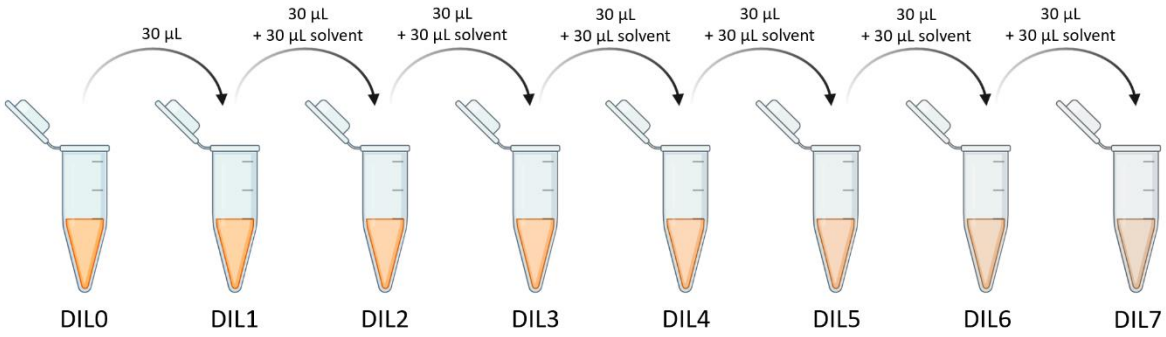

Fig SI-1.3.1. Dilution series used during optimization of the dilution factor for the extracellular fraction of HepaRG sample extracts. Graphical icons were provided by BioRender, license No. 2641-5211.

After data-acquisition, data-preprocessing consisted of peak picking, alignment, missing value imputation and solvent blank subtraction (section 2.6.). The mean of replicate intensity values was calculated and $\log_{10}$ transformed. For each feature, the Pearson correlation coefficients (r) were calculated based on the intensity for each combination of four or more consecutive dilution factors. Features with $r > 0.9$ for at least one of the combinations of ≥ 4 consecutive dilution factors were kept. After excluding the features with low Pearson correlation coefficients ≤ 0.9, the mean intensity of features was plotted per dilution factor (Fig. SI-1.3.2). For the apolar fraction (Fig. SI-1.3.2.A) in ESI (-), there is only a small increase in mean intensity going from the highest dilution to dilution 3, indicating a high number of features at low intensity. In ESI (+), dilution 0 (i.e., the most concentrated sample) showed only a small increase in mean intensity compared to the other dilutions. This could indicate a larger number of features close to the detector saturation level in comparison to dilution 1. For the polar fraction (Fig. SI-1.3.2.B), no indications for detector saturation could be observed in ESI (+). However, in ESI (-), dilution 0 showed a lower mean intensity in comparison to dilution 1. Based on these results, dilution 2 or dilution 1 would be suitable concentrations for the apolar

fraction, while dilution 2 is preferred for the polar fraction. The sample preparation was adapted accordingly as explained in SI-1.2.

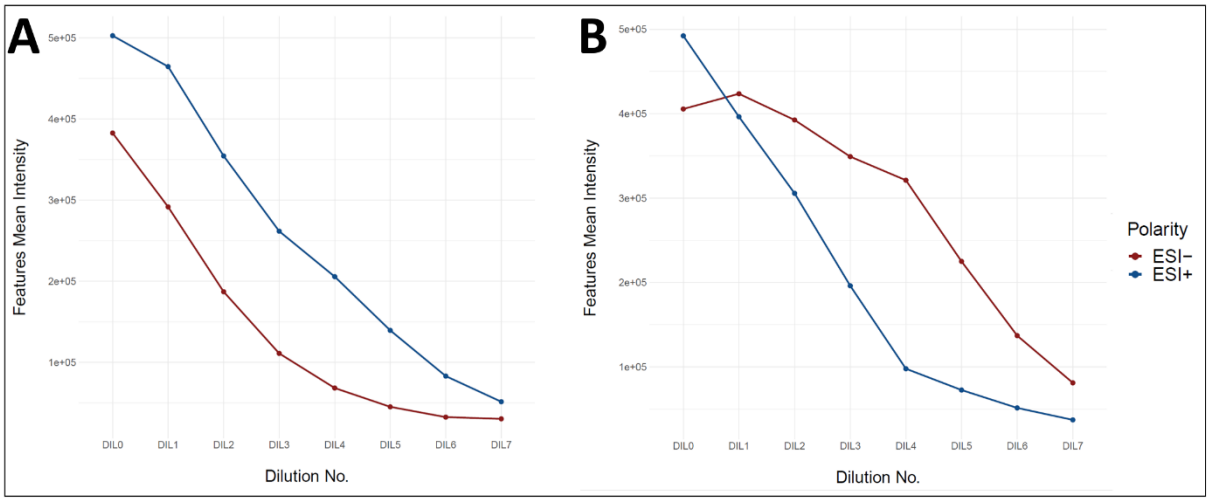

Fig SI-1.3.2. Mean intensity of features in relation to the dilution factor of the extracellular apolar (A) and polar (B) fractions of HepaRG cells.

Section 2. Data acquisition

Table SI-2.1. Data acquisition parameters per sample fraction. For mobile phase compositions, modifier concentrations were calculated based on the volume of the aqueous fraction. For polar methods (ESI (+) and ESI (-)), additional MS2 runs were acquired using one collision energy at a time (10, 20 or 40 eV) with a maximum of 12 precursors per scan cycle (*). In addition, interesting features selected after the first exposure experiments were used to build a fragmentation target list, which was used during the validation experiments. ESI: Electrospray ionization. LC: Liquid chromatography. QToF: Quadrupole-time-of-flight. DTIM: Drift tube ion mobility. BEH: Ethylene bridged hybrid. UPLC: Ultra performance liquid chromatography. MeOH: Methanol. ACN: Acetonitrile. IPA: Isopropanol.

Sample fraction	Polar	Polar	Apolar	Apolar
ESI mode	ESI (+)	ESI (-)	ESI (+)	ESI (-)
LC system	Agilent 1290 Infinity	Agilent 1290 Infinity	Agilent 1290 Infinity II	Agilent 1290 Infinity II
Detector	Agilent 6530 QToF	Agilent 6530 QToF	Agilent 6560 (DTIM)-QToF	Agilent 6560 (DTIM)-QToF
Column	iHILIC-Fusion	iHILIC-Fusion(P)	ACQUITY UPLC BEH C18	ACQUITY UPLC BEH C18
Column dimensions	100 x 2.1 mm, 1.8 µm	100 x 2.1 mm, 5 µm	150 x 2.1 mm, 1.7 µm	150 x 2.1 mm, 1.7 µm
Mobile phase A	10 mM NH_4COOH + 0.1% (v/v) HCOOH in H_2O/MeOH (9/1, v/v)	2 mM NH_4COOCH_3 + 2 mM $(NH_4)_2CO_3$ in H_2O	5 mM NH_4COOCH_3 + 0.1% (v/v) $HCOOCH_3$ in H_2O/ACN (7/3, v/v)	5 mM NH_4COOCH_3 in H_2O/ACN (7/3, v/v)
Mobile phase B	ACN	ACN/MeOH (9/1, v/v)	5 mM NH_4COOCH_3 + 0.1% (v/v) $HCOOCH_3$ in H_2O/ACN/IPA (2/10/88, v/v/v)	5 mM NH_4COOCH_3 in H_2O/ACN/IPA (2/10/88, v/v/v)
Flow rate (mL/min)	0.25	0.20	0.20	0.20
Gradient	Min - %B 0 – 95 4 – 95 12.5 – 60 20 – 60 21 – 95 26 – 95	Min - %B 0 – 95 1 – 95 10 – 20 14 – 20 15 – 95 20 – 95	Min - %B 0 – 15 2 – 15 3 – 30 5 – 60 8 – 60 20 – 100 30 – 100 35 – 15 40 – 15	Min - %B 0 – 15 2 – 15 3 – 30 5 – 60 8 – 60 20 – 100 30 – 100 35 – 15 40 – 15
Injection volume (µL)	3	3	3	2
Autosampler temperature (°C)	4	4	4	4
Column temperature	60	25, bypassing heat exchanger	60	60

Table SI-2.1. Continuation.

Sample fraction	Polar	Polar	Apolar	Apolar
Nozzle voltage (V)	0	0	500	500
Capillary voltage (V)	2000	2000	3500	3750
Fragmentor voltage (V)	150	100	200	200
Drying gas	Nitrogen	Nitrogen	Nitrogen	Nitrogen
Sheath gas	Nitrogen	Nitrogen	Nitrogen	Nitrogen
Drying gas temperature (°C)	250	250	325	350
Sheath gas temperature (°C)	350	350	325	350
Drying gas flow (L/min)	8	10	8	8
Sheath gas flow (L/min)	11	10	8	8
Nebulizer gas pressure (psig)	45	45	30	30
MS1 range (*m/z*)	60-1200	60-1200	100-1500	100-1500
MS1 acquisition mode	Profile	Profile	Profile	Profile
MS1 scan rate (spectra/s)	2	2	4	4
MS2 mass range (*m/z*)	40-1000	40-1000	60-1200	60-1200
MS2 acquisition mode	Profile (auto MS/MS)	Profile (auto MS/MS)	Profile (auto MS/MS with iterative exclusion)	Profile (auto MS/MS with iterative exclusion)
MS2 scan rate (spectra/s)	6	6	6	6
Max precursors/scan cycle	4*	4*	4	4
Collision energy (eV)	10-20-40*	10-20-40*	10-20-40	10-20-40
Quad width	Small (1.3 amu)	Small (1.3 amu)	Small (1.3 amu)	Small (1.3 amu)
DTIM drift entrance voltage (V)	/	/	1221	1273
DTIM drift exit voltage (V)	/	/	200	300
DTIM rear funnel entrance voltage (V)	/	/	200	216
DTIM rear funnel exit voltage (V)	/	/	49	47
DTIM single pulse trap filling time (µs)	/	/	30,000	30,000
DTIM single pulse trap release time (µs)	/	/	200	200
DTIM 4-bit multiplexing trap filling time (µs)	/	/	3,000	3,000
DTIM 4-bit multiplexing trap release time (µs)	/	/	200	200

Section 3. MS-DIAL parameters

Converted data files (.mzML format) were imported and processed using MS-DIAL software version 4.6. The following parameters were used for peak detection and alignment (Table SI-3.1).

Table SI-3.1. MS-DIAL parameters used for peak detection and alignment. ESI: Electrospray ionization. RT: Retention time.

Sample fraction	Polar	Polar	Apolar	Apolar
ESI mode	ESI (+)	ESI (-)	ESI (+)	ESI (-)
Mass range (Da)	60-1200	60-1200	100-1500	100-1500
RT range (min)	0.5-22	0.5-19.5	0.5-30	0.5-30
Accurate mass tolerance (MS1) (Da)	0.01	0.01	0.01	0.01
Accurate mass tolerance (MS2) (Da)	0.05	0.05	0.05	0.05
Maximum charged number	1	1	1	1
Smoothing method	linear weighted moving average	linear weighted moving average	linear weighted moving average	linear weighted moving average
Scans smoothing level	3	3	3	3
Scans minimum peak width	5	5	5	5
Mass slice width (Da)	0.1	0.1	0.1	0.1
Sigma window value	0.5	0.5	0.5	0.5
RT tolerance alignment (Da)	0.2	0.2	0.15	0.15
MS1 tolerance alignment (Da)	0.015	0.015	0.01	0.01
Gap filling	Yes	Yes	Yes	Yes
Adduct ion setting	$[M+H]^+$, $[M+NH4]^+$, $[M+Na]^+$, $[M-H2O+H]^+$	$[M-H]^-$, $[M-H2O-H]^-$, $[M+HCOO]^-$, $[M+CH3COO]^-$	$[M+H]^+$, $[M+NH4]^+$, $[M+Na]^+$, $[M-H2O+H]^+$	$[M-H]^-$, $[M-H2O-H]^-$, $[M+HCOO]^-$, $[M+CH3COO]^-$

Section 4. Neutral red uptake assay

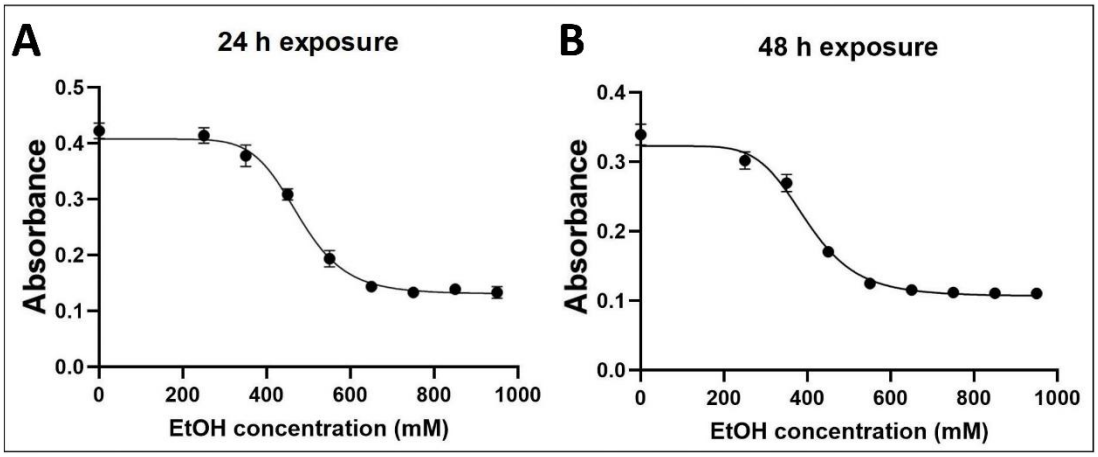

Fig. SI-4.1. Absorbance measured during neutral red uptake assay for 24 h (A) and 48 h (B) of ethanol exposure. Cells were incubated using eight different ethanol concentrations (n = 3).

Section 5. Data processing

Table SI-5.1. Median relative standard deviation (mRSD) of the intensity of LC-MS features for each analytical platform and sample group of the intracellular HepaRG fraction. mRSD values were calculated after deisotoping and blank subtraction. B1: Batch 1. B2: Batch 2. LIP+: Lipidomics in positive electrospray ionization mode. LIP-: Lipidomics in negative electrospray ionization mode. MET+: Metabolomics in positive electrospray ionization mode. MET-: Metabolomics in negative electrospray ionization mode.

	QC	Control	IC_{10}	1/10 IC_{10}
B1-24h-LIP+	12.8	17.8	26.0	20.1
B2-24h-LIP+	12.8	22.1	22.1	24.1
B1-48h-LIP+	9.3	17.8	22.7	25.6
B2-48h-LIP+	14.6	23.8	21.7	23.1
B1-24h-LIP-	11.2	22.9	32.4	25.7
B2-24h-LIP-	10.4	13.8	17.0	18.5
B1-48h-LIP-	10.8	25.9	21.4	28.3
B2-48h-LIP-	10.7	25.2	20.5	27.4
B1-24h-MET+	21.1	27.5	28.3	28.3
B2-24h-MET+	11.8	19.9	16.9	17.8
B1-48h-MET+	13.0	21.0	21.6	19.6
B2-48h-MET+	13.4	22.5	23.4	20.2
B1-24h-MET-	19.4	22.7	25.9	21.0
B2-24h-MET-	19.3	27.1	24.8	25.8
B1-48h-MET-	16.0	21.6	22.7	19.1
B2-48h-MET-	17.2	24.5	18.5	25.8

Table SI-5.2. Median relative standard deviation (mRSD) of the intensity of LC-MS features for each analytical platform and sample group of the extracellular HepaRG fraction. mRSD values were calculated after deisotoping and blank subtraction. B1: Batch 1. B2: Batch 2. LIP+: Lipidomics in positive electrospray ionization mode. LIP-: Lipidomics in negative electrospray ionization mode. MET+: Metabolomics in positive electrospray ionization mode. MET-: Metabolomics in negative electrospray ionization mode.

	QC	Control	IC_{10}	1/10 IC_{10}
B1-24h-LIP+	11.0	20.5	25.4	20.3
B2-24h-LIP+	13.6	22.4	19.6	20.1
B1-48h-LIP+	10.7	19.6	23.2	17.7
B2-48h-LIP+	12.9	23.3	29.0	19.3
B1-24h-LIP-	10.1	21.6	16.1	22.0
B2-24h-LIP-	11.2	23.6	16.7	22.6
B1-48h-LIP-	10.3	14.8	19.7	18.0
B2-48h-LIP-	10.0	15.8	20.7	18.4
B1-24h-MET+	12.4	16.2	15.9	17.7
B2-24h-MET+	13.5	15.1	15.5	16.3
B1-48h-MET+	12.2	14.4	15.6	15.7
B2-48h-MET+	13.7	18.1	17.9	18.9
B1-24h-MET-	20.6	23.4	22.9	20.9
B2-24h-MET-	20.0	22.9	20.2	21.2
B1-48h-MET-	20.5	20.1	24.4	20.8
B2-48h-MET-	26.2	26.1	27.7	26.3

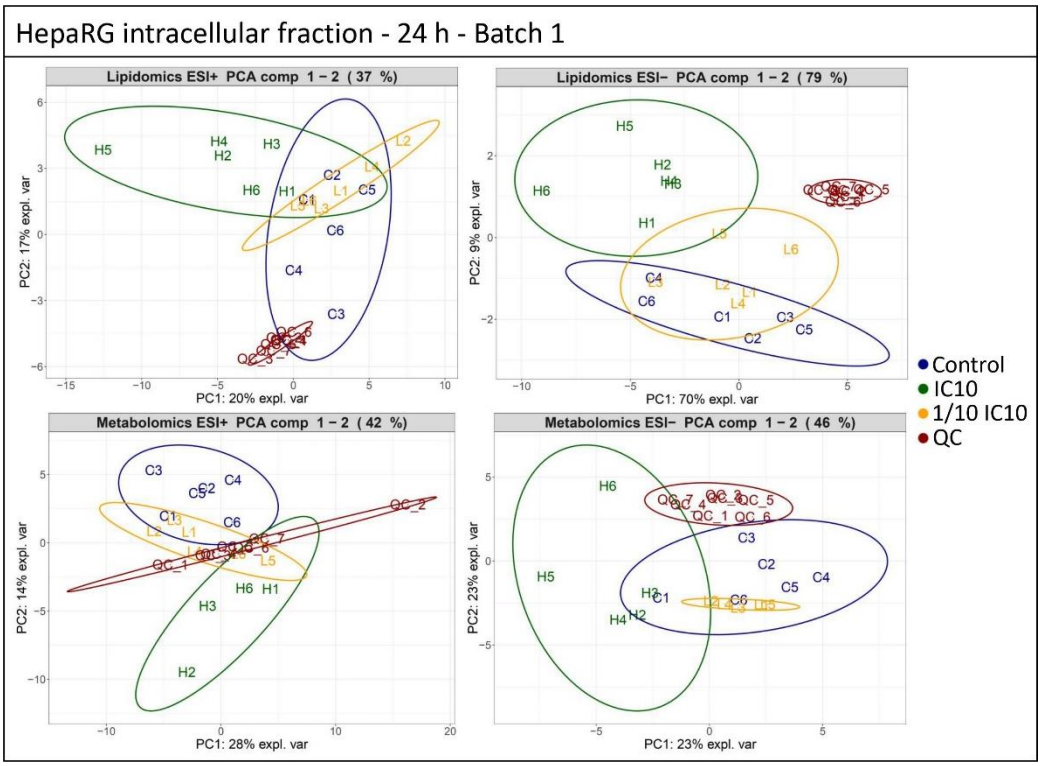

Fig. SI-5.1. Principal component analysis plots of the intracellular fraction of HepaRG cells of batch 1 after 24 h exposure to ethanol. ESI+ and ESI- refer to electrospray ionization in positive and negative modes, respectively.

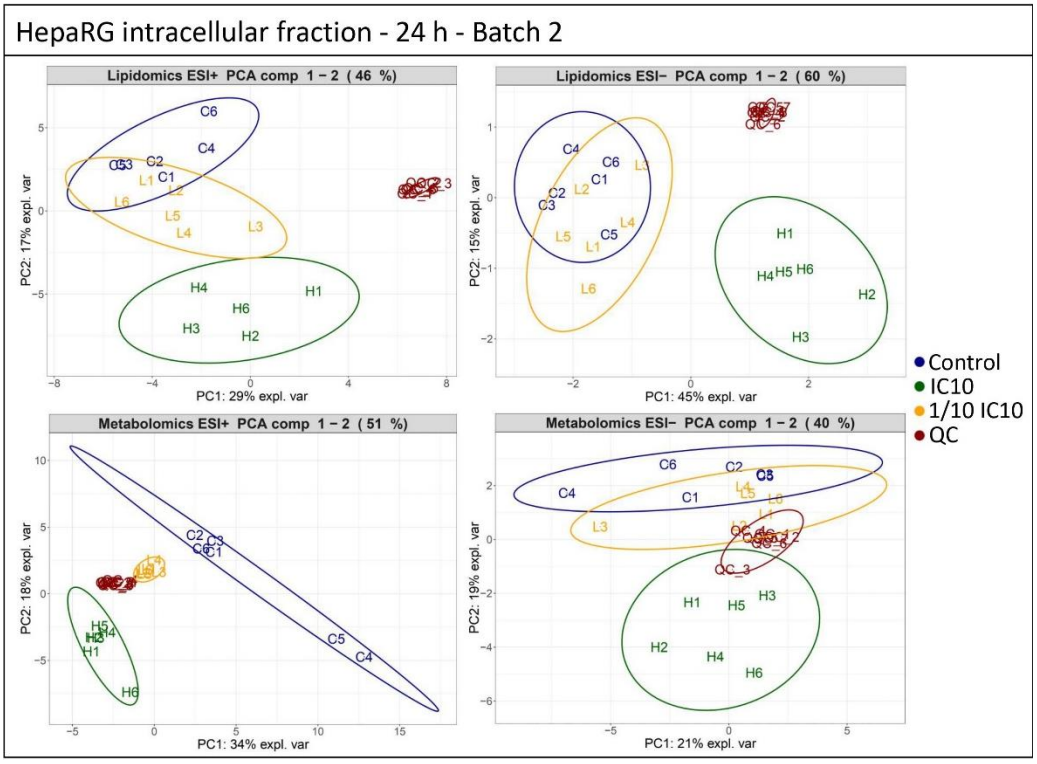

Fig. SI-5.2. Principal component analysis plots of the intracellular fraction of HepaRG cells of batch 2 after 24 h exposure to ethanol. ESI+ and ESI- refer to electrospray ionization in positive and negative modes, respectively.

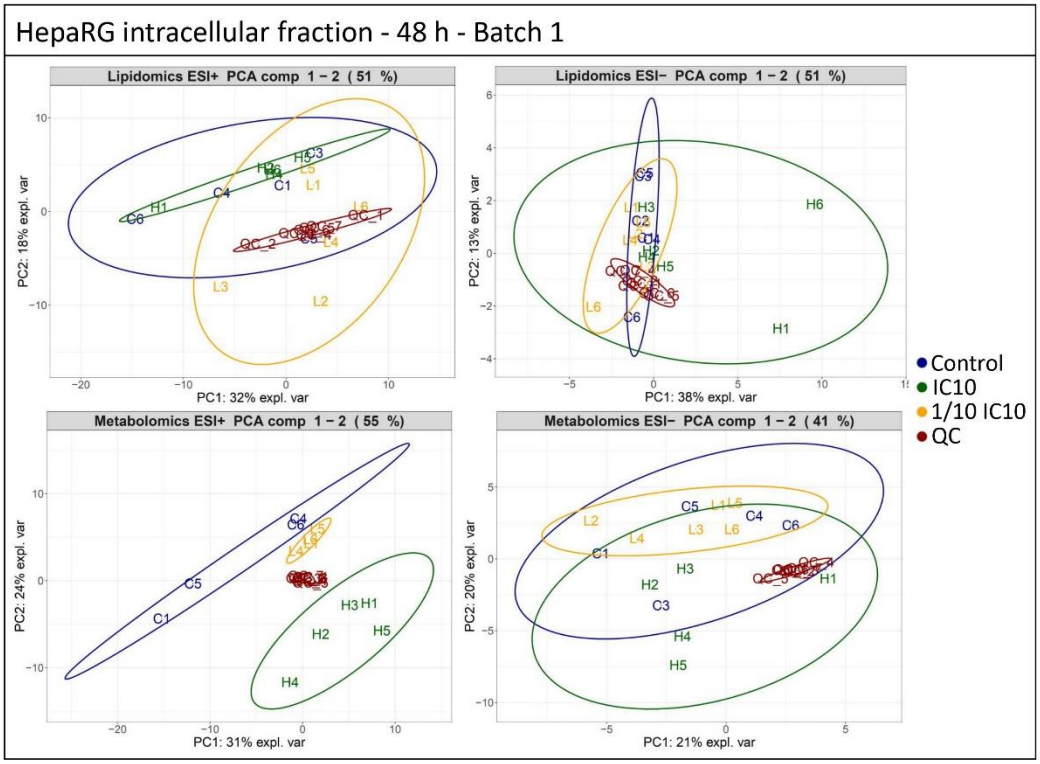

Fig. SI-5.3. Principal component analysis plots of the intracellular fraction of HepaRG cells of batch 1 after 48 h exposure to ethanol. ESI+ and ESI- refer to electrospray ionization in positive and negative modes, respectively.

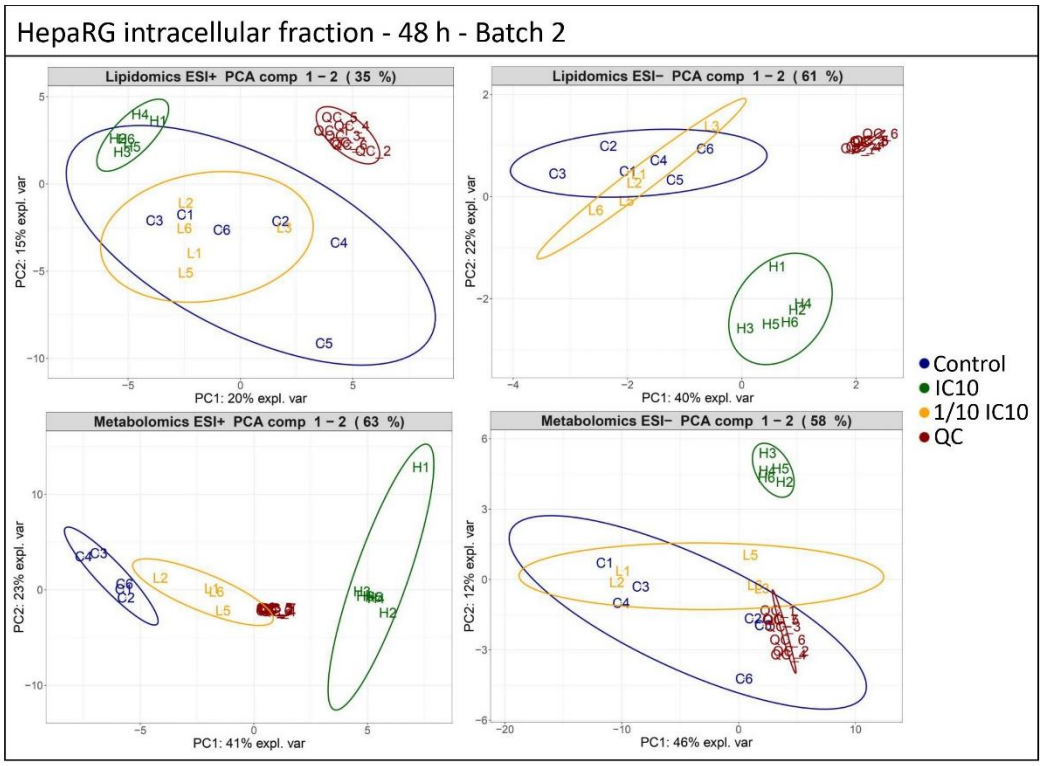

Fig. SI-5.4. Principal component analysis plots of the intracellular fraction of HepaRG cells of batch 2 after 48 h exposure to ethanol. ESI+ and ESI- refer to electrospray ionization in positive and negative modes, respectively.

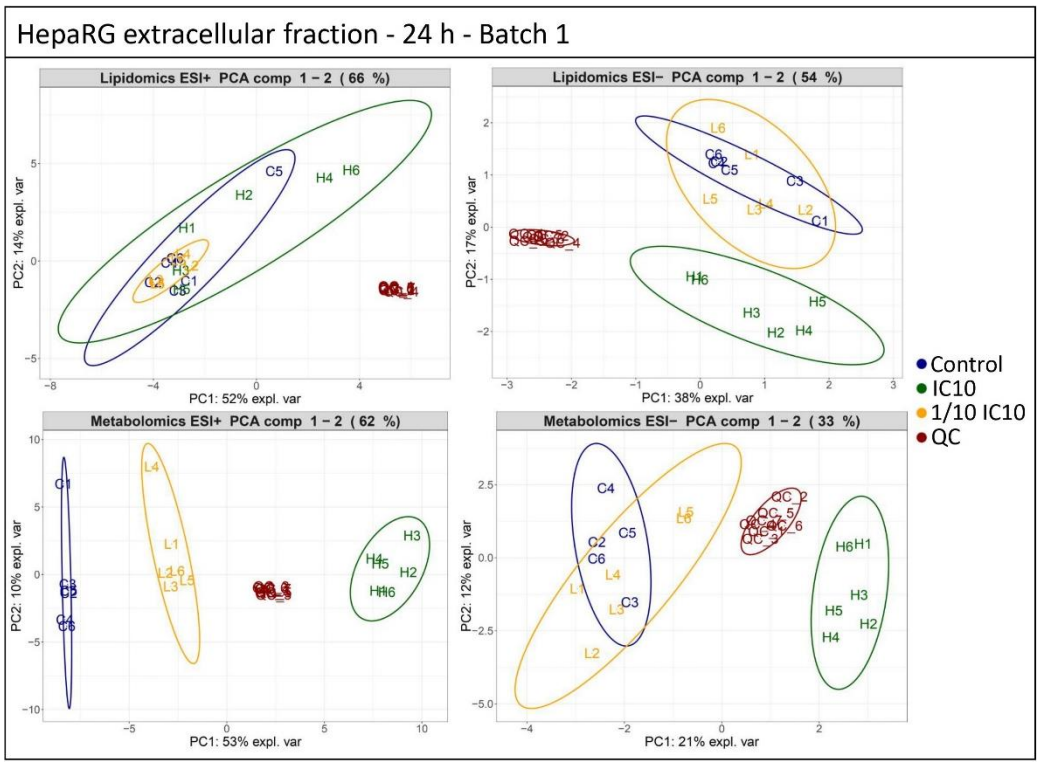

Fig. SI-5.5. Principal component analysis plots of the extracellular fraction of HepaRG cells of batch 1 after 24 h exposure to ethanol. ESI+ and ESI- refer to electrospray ionization in positive and negative modes, respectively.

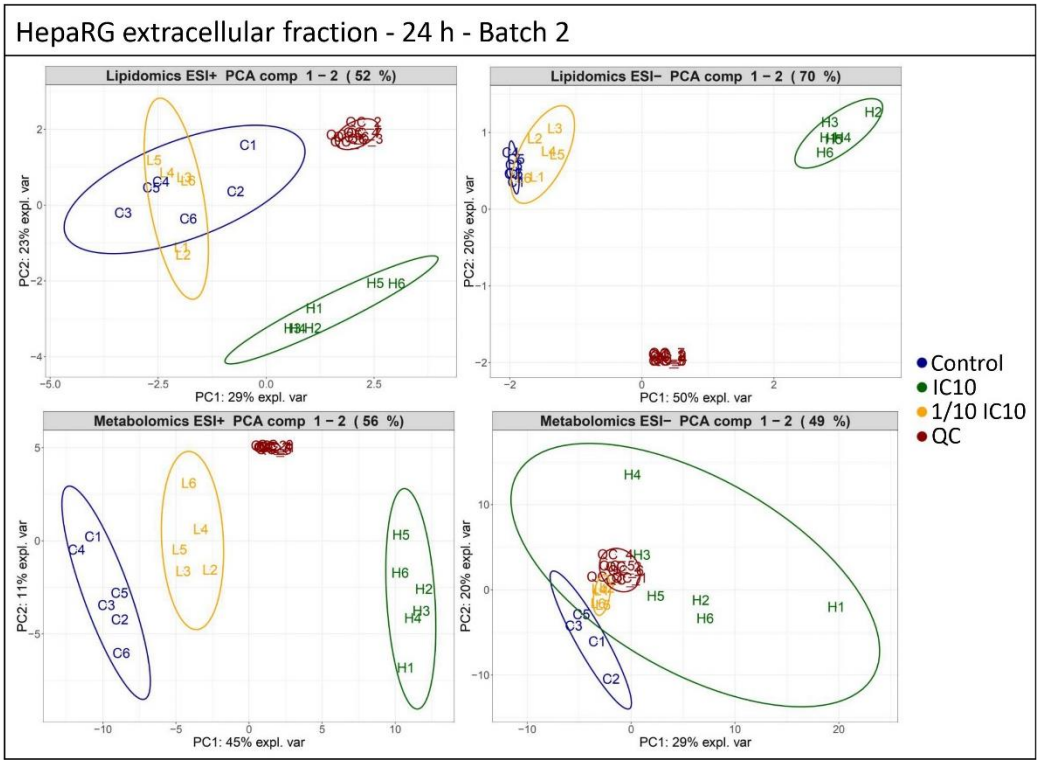

Fig. SI-5.6. Principal component analysis plots of the extracellular fraction of HepaRG cells of batch 2 after 24 h exposure to ethanol. ESI+ and ESI- refer to electrospray ionization in positive and negative modes, respectively.

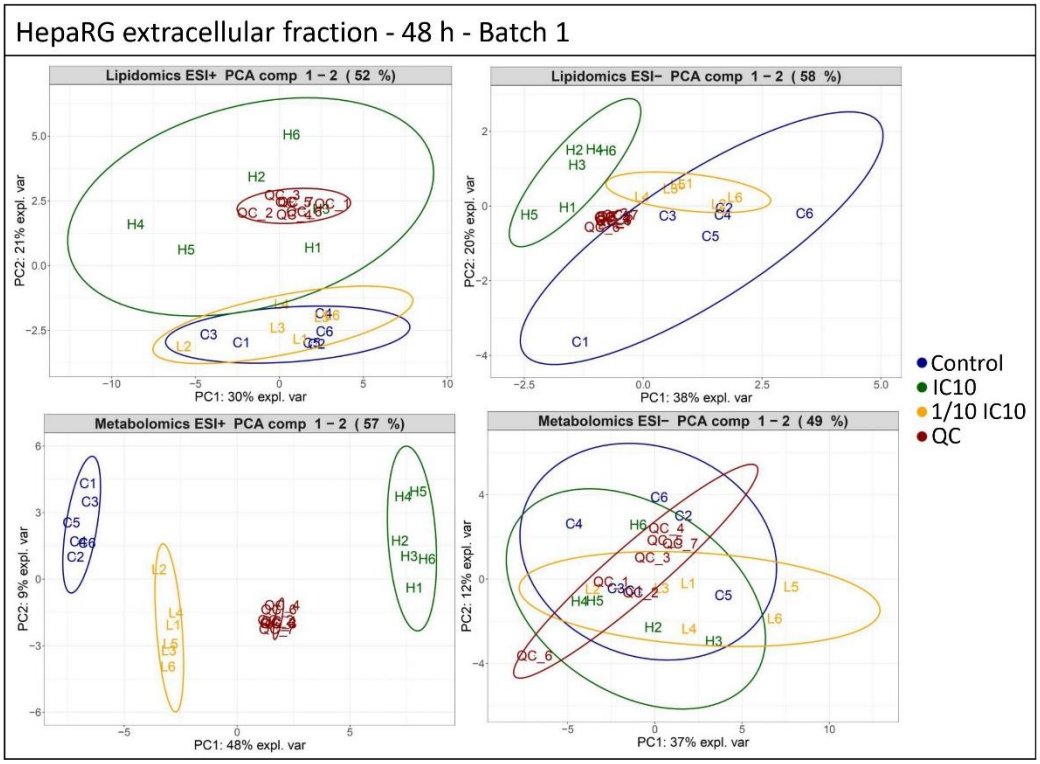

Fig. SI-5.7. Principal component analysis plots of the extracellular fraction of HepaRG cells of batch 1 after 48 h exposure to ethanol. ESI+ and ESI- refer to electrospray ionization in positive and negative modes, respectively.

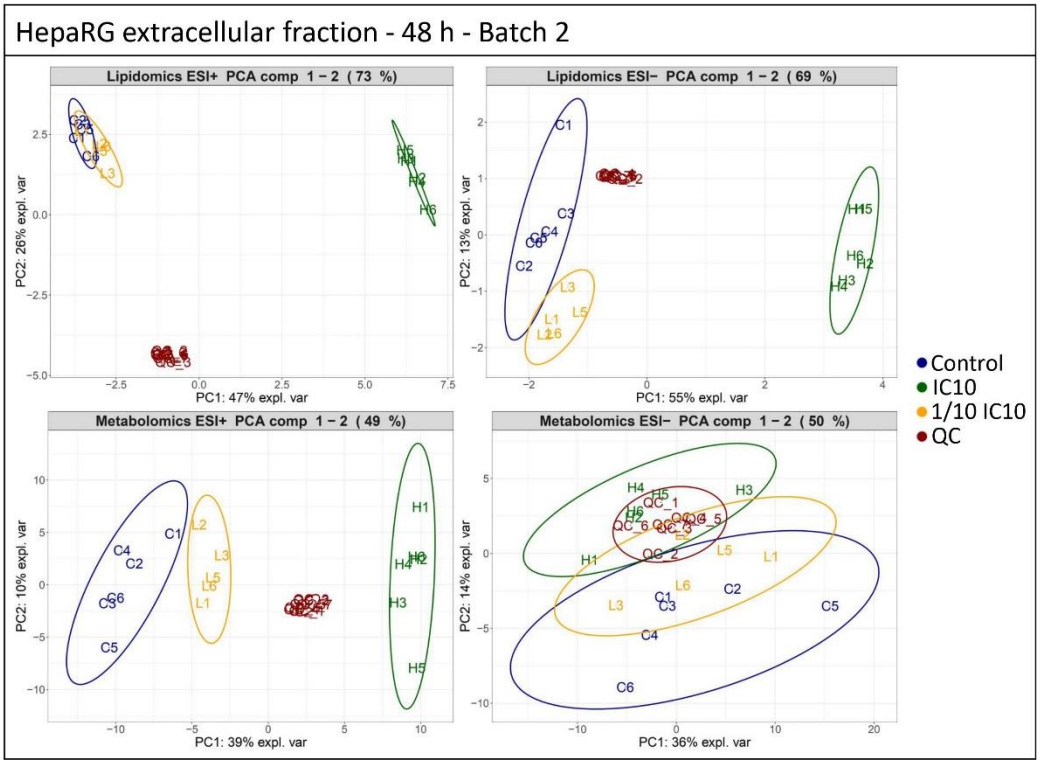

Fig. SI-5.8. Principal component analysis plots of the extracellular fraction of HepaRG cells of batch 2 after 48 h exposure to ethanol. ESI+ and ESI- refer to electrospray ionization in positive and negative modes, respectively.

Table SI-5.3. Evaluation parameters of multivariate statistical models for the intracellular fraction after exposure to the IC_{10} concentration of ethanol for 24 h an 48 h. R^2, Q^2, R^2_{PERM} and Q^2_{PERM} (calculated after 1000 random permutations) were selected for evaluation of the PLS-DA model, while the area under the curve (AUC) was selected for evaluation of the random forest classification model. B1: Batch 1. B2: Batch 2. LIP+: Lipidomics in positive electrospray ionization mode. LIP-: Lipidomics in negative electrospray ionization mode. MET+: Metabolomics in positive electrospray ionization mode. MET-: Metabolomics in negative electrospray ionization mode.

	R^2	Q^2	R^2_{PERM}	Q^2_{PERM}	AUC
B1-24h-LIP+	0.97	0.85	0.00	0.00	1.00
B2-24h-LIP+	1.00	0.96	0.01	0.00	1.00
B1-48h-LIP+	0.89	0.50	0.01	0.04	0.93
B2-48h-LIP+	0.96	0.85	0.00	0.00	1.00
B1-24h-LIP-	0.98	0.82	0.01	0.00	1.00
B2-24h-LIP-	0.99	0.90	0.03	0.00	1.00
B1-48h-LIP-	1.00	0.95	0.01	0.00	1.00
B2-48h-LIP-	0.91	0.86	0.02	0.00	1.00
B1-24h-MET+	1.00	0.86	0.01	0.01	1.00
B2-24h-MET+	0.99	0.95	0.00	0.00	1.00
B1-48h-MET+	0.93	0.86	0.01	0.01	1.00
B2-48h-MET+	0.95	0.92	0.00	0.00	1.00
B1-24h-MET-	0.87	0.78	0.04	0.00	1.00
B2-24h-MET-	0.95	0.87	0.00	0.00	1.00
B1-48h-MET-	0.89	0.75	0.02	0.01	1.00
B2-48h-MET-	0.96	0.88	0.00	0.00	1.00

Table SI-5.4. Evaluation parameters of multivariate statistical models for the intracellular fraction after exposure to the 1/10 of the IC_{10} concentration of ethanol for 24 h and 48 h. R^2, Q^2, R^2_{PERM} and Q^2_{PERM} (calculated after 1000 random permutations) were selected for evaluation of the PLS-DA model, while the area under the curve (AUC) was selected for evaluation of the random forest classification model. B1: Batch 1. B2: Batch 2. LIP+: Lipidomics in positive electrospray ionization mode. LIP-: Lipidomics in negative electrospray ionization mode. MET+: Metabolomics in positive electrospray ionization mode. MET-: Metabolomics in negative electrospray ionization mode.

	R^2	Q^2	R^2_{PERM}	Q^2_{PERM}	AUC
B1-24h-LIP+	0.83	0.37	0.05	0.03	0.75
B2-24h-LIP+	0.99	0.73	0.13	0.02	0.97
B1-48h-LIP+	0.99	0.70	0.12	0.08	0.97
B2-48h-LIP+	1.00	0.15	0.94	0.75	0.62
B1-24h-LIP-	0.54	0.20	0.27	0.05	0.83
B2-24h-LIP-	1.00	0.83	0.03	0.00	0.88
B1-48h-LIP-	0.99	0.71	0.17	0.07	0.77
B2-48h-LIP-	0.95	0.76	1.00	0.86	0.56
B1-24h-MET+	1.00	0.74	0.68	0.12	0.91
B2-24h-MET+	0.63	0.49	0.16	0.01	0.92
B1-48h-MET+	0.99	0.50	0.32	0.06	0.61
B2-48h-MET+	0.96	0.66	0.09	0.01	0.65
B1-24h-MET-	1.00	0.89	0.01	0.00	0.80
B2-24h-MET-	1.00	0.57	0.06	0.03	0.86
B1-48h-MET-	0.84	0.30	0.18	0.07	0.79
B2-48h-MET-	1.00	0.27	0.71	0.79	0.31

Table SI-5.5. Evaluation parameters of multivariate statistical models for the extracellular fraction after exposure to the IC_{10} concentration of ethanol for 24 h and 48 h. R^2, Q^2, R^2_{PERM} and Q^2_{PERM} (calculated after 1000 random permutations) were selected for evaluation of the PLS-DA model, while the area under the curve (AUC) was selected for evaluation of the random forest classification model. B1: Batch 1. B2: Batch 2. LIP+: Lipidomics in positive electrospray ionization mode. LIP-: Lipidomics in negative electrospray ionization mode. MET+: Metabolomics in positive electrospray ionization mode. MET-: Metabolomics in negative electrospray ionization mode.

	R^2	Q^2	R^2_{PERM}	Q^2_{PERM}	AUC
B1-24h-LIP+	0.94	0.89	0.00	0.00	1.00
B2-24h-LIP+	0.94	0.89	0.00	0.00	1.00
B1-48h-LIP+	0.90	0.78	0.00	0.00	1.00
B2-48h-LIP+	0.90	0.78	0.00	0.00	0.99
B1-24h-LIP-	0.95	0.93	0.00	0.00	1.00
B2-24h-LIP-	0.95	0.93	0.00	0.00	1.00
B1-48h-LIP-	0.91	0.79	0.00	0.00	1.00
B2-48h-LIP-	0.91	0.79	0.00	0.00	1.00
B1-24h-MET+	0.97	0.95	0.00	0.00	1.00
B2-24h-MET+	0.97	0.95	0.00	0.00	1.00
B1-48h-MET+	0.96	0.91	0.00	0.00	1.00
B2-48h-MET+	0.96	0.91	0.00	0.00	1.00
B1-24h-MET-	0.94	0.70	0.14	0.00	1.00
B2-24h-MET-	0.94	0.70	0.14	0.00	0.99
B1-48h-MET-	0.99	0.92	0.01	0.00	0.94
B2-48h-MET-	0.99	0.92	0.01	0.00	0.95

Table SI-5.6. Evaluation parameters of multivariate statistical models for the extracellular fraction after exposure to the 1/10 of the IC_{10} concentration of ethanol for 24 h and 48 h. R^2, Q^2, R^2_{PERM} and Q^2_{PERM} (calculated after 1000 random permutations) were selected for evaluation of the PLS-DA model, while the area under the curve (AUC) was selected for evaluation of the random forest classification model. B1: Batch 1. B2: Batch 2. LIP+: Lipidomics in positive electrospray ionization mode. LIP-: Lipidomics in negative electrospray ionization mode. MET+: Metabolomics in positive electrospray ionization mode. MET-: Metabolomics in negative electrospray ionization mode.

	R^2	Q^2	R^2_{PERM}	Q^2_{PERM}	AUC
B1-24h-LIP+	0.70	0.19	0.27	0.08	0.60
B2-24h-LIP+	0.62	0.40	0.17	0.01	0.87
B1-48h-LIP+	0.99	0.77	0.03	0.01	0.87
B2-48h-LIP+	0.86	0.70	0.04	0.01	0.86
B1-24h-LIP-	0.96	0.28	0.13	0.09	0.66
B2-24h-LIP-	0.25	0.10	0.29	0.03	0.69
B1-48h-LIP-	0.69	0.25	0.02	0.04	0.96
B2-48h-LIP-	0.70	0.22	0.03	0.03	0.84
B1-24h-MET+	0.99	0.71	0.15	0.01	0.93
B2-24h-MET+	1.00	0.83	0.16	0.00	0.99
B1-48h-MET+	0.98	0.88	0.04	0.00	1.00
B2-48h-MET+	1.00	0.79	0.34	0.03	0.88
B1-24h-MET-	0.89	0.15	0.31	0.13	0.55
B2-24h-MET-	0.99	0.46	0.02	0.04	0.85
B1-48h-MET-	1.00	0.92	0.15	0.00	0.75
B2-48h-MET-	1.00	0.59	1.00	0.88	0.75

Section 6. Metabolic changes in the intracellular fraction of HepaRG cells

Table SI-6.1. Annotated metabolites that showed alterations after ethanol exposure in the intracellular fraction of HepaRG cells. Classes were adopted from LIPID MAPS for lipids and from HMDB for polar metabolites. CCS errors were calculated comparing obtained experimental single-field $^{DT}CCS_{N2}$ with experimental database values from CCS compendium ([I]), CCSbase ([II]), MS-DIAL internal lipidomic library v. 4.6 ([III]) or *in silico* generated CCS values using AllCCS ([IV]).[4–7] Annotation levels refer to the confidence levels of Schymanski et al.[8]

Bulk name	Species name	Class	Formula	Ionization species	*m/z*	RT (min)	$^{DT}CCS_{N2}$ (Å^2)	Annotation level	Mass error (ppm)	CCS error (%)	IC_{10} exposure		1/10 IC_{10} exposure	
											24h	48h	24h	48h
Acetylcarnitine	Acetylcarnitine	Fatty esters	C9H17NO4	[M+H]+	204.1223	13.6	-	1	3.8	-	↓	↓		
Acetylcholine	Acetylcholine	Organonitrogen compounds	C7H16NO2+	[M]+	146.1185	9.3	-	1	-2.7	-	↓	↓		
Carnitine	Carnitine	Organonitrogen compounds	C7H15NO3	[M+H]+	162.1130	13.3	-	1	-3.2	-	↓	↓		
Creatine	Creatine	Carboxylic acids and derivatives	C4H9N3O2	[M+H]+ [M+Na]+	132.0768 154.0563	13.0 13.0	-	1	-0.2 15.7	-	↓ ↓	↓	↓ ↓	↓
Ethoxylated phosphorylcholine	2-[Ethoxy(hydroxy)phosphoryl]oxyethyl-trimethylazanium	Organonitrogen compounds	C7H19NO4P+	[M]+	212.1061	13.6	-	2b	4.2	-	↑	↑	↑	↑
Glycerophosphocholine	Glycerophosphocholine	Glycerophosphocholines	C8H20NO6P	[M+H]+	258.1096	14.3	-	2a	1.8	-	↓	↓	↓	↓
O-adipoylcarnitine	O-adipoylcarnitine	Fatty esters	C13H23NO6	[M+H]+	290.1588	11.2	-	2a	3.4	-	↑	↑	↑	↑
O-phosphoethanolamine	O-phosphoethanolamine	Organic phosphoric acids and derivatives	C2H8NO4P	[M-H]-	140.0112	6.4	-	1	4.5	-	↑	↑		
Pantothenic acid	Pantothenic acid	Organooxygen compounds	C9H17NO5	[M+H]+	220.1171	4.9	-	1	4.0	-	↓	↓		
Phenylacetylglutamine	Phenylacetylglutamine	Carboxylic acids and derivatives	C13H16N2O4	[M+H]+	265.1174	8.3	-	1	3.3	-	↓	↓		
S-Adenosylmethionine	S-Adenosylmethionine	5'-deoxyribonucleosides	C15H22N6O5S	[M+H]+	399.1430	17.6	-	2a	3.7	-	↓	↓	↓	↓
Taurine	Taurine	Organic sulfonic acids and derivatives	C2H7NO3S	[M-H]-	124.0073	5.8	-	1	-1.0	-	↓	↓		
Cer 34:2;2O	Cer 18:2;O2/16:0	Ceramides	C34H65NO3	[M-H]-	534.4894	16.9	234.0	2a	0.5	0.0[IV]	↓	↓		
Cer 40:2;2O	Cer 18:2;O2/22:0	Ceramides	C40H77NO3	[M+H]+	620.5985	19.1	269.0	2a	1.5	-2.0[I]	↓	↓		
Cer 42:3;2O	Cer 18:2;O2/24:1	Ceramides	C42H79NO3	[M+H-H2O]+	628.6005	19.1	273.3	2a	-3.5	-0.1[I]	↓	↓		
DG 32:1	DG 16:0_16:1	Diradylglycerols	C35H66O5	[M+NH4]+	584.5254	18.2	254.6	2a	-1.0	-0.4[II]	↑	↑	↑	↑
DG 34:2	DG 16:0_18:2	Diradylglycerols	C37H68O5	[M+NH4]+	610.5422	18.4	258.7	2a	-2.7	0.6[II]	↑	↑		
DG 34:2	DG 16:1_18:1	Diradylglycerols	C37H68O5	[M+NH4]+	610.5422	18.4	258.4	2a	2.7	0.0[II]	↑	↑		
DG 36:2	DG 18:1/18:1	Diradylglycerols	C39H72O5	[M+NH4]+	638.5749	18.9	264.9	2a	-4.8	1.1[II]		↑		
DG 36:3	DG 18:1_18:2	Diradylglycerols	C39H70O5	[M+NH4]+	636.5568	18.4	260.9	2a	-1.1	0.6[II]	↑	↑		

Table SI-6.1. Continuation.

Bulk name	Species name	Class	Formula	Ionization species	*m/z*	RT (min)	$^{DT}CCS_{N2}$ (Å^2)	Anno-tation level	Mass error (ppm)	CCS error (%)	IC_{10} exposure		1/10 IC_{10} exposure	
											24h	48h	24h	48h
LBPA 36:2	LBPA 18:1/18:1	Glycerophosphoglycer-ols	C42H79O10P	[M+Na]+	797.5300	14.9	288.0	2a	0.4	0.7^{IV}	↓	↓		
LPC 26:0	LPC 26:0	Glycerophosphocho-lines	C34H70NO7P	[M+H]+	636.4999	15.0	269.0	2a	5.7	0.2^{IV}	↓	↓		
LPC 28:0	LPC 28:0	Glycerophosphocho-lines	C36H74NO7P	[M+H]+ [M+Na]+	664.5264 686.5085	16.3 16.2	275.3 277.6	2a	1.8 1.5	0.6^{IV} 1.2^{IV}	↓ ↓	↓ ↓	↓	↓
LPC 28:1	LPC 28:1	Glycerophosphocho-lines	C36H72NO7P	[M+H]+	662.5116	16.1	273.4	2a	0.4	1.7^{IV}	↓	↓		
PC 28:0		Glycerophosphocholines	C36H72NO8P	[M+H]+	678.5062	15.5	274.4	3	1.0	0.7^{I}	↓	↓		
PC 30:0	PC 16:0_14:0	Glycerophosphocholines	C38H76NO8P	[M+CH3COO]- [M+H]+ [M+Na]+	764.5467 706.5371 728.5223	16.6 16.6 16.6	284.7 279.4 282.3	2a	2.5 1.5 3.0	2.5^{III} -0.1^{II} 2.5^{II}	↓ ↓ ↓	↓ ↓ ↓		
PC 30:1		Glycerophosphocholines	C38H74NO8P	[M+H]+	704.5240	15.6	276.1	3	-2.2	0.0^{II}	↓	↓	↓	↓
PC 30:2		Glycerophosphocholines	C38H72NO8P	[M+H]+	702.5050	14.6	272.2	3	2.7	-0.6^{II}	↓	↓		
PC 31:0		Glycerophosphocholines	C39H78NO8P	[M+H]+	720.5532	17.0	283.9	3	0.8	0.2^{II}	↓	↓		
PC 32:0	PC 16:0/16:0	Glycerophosphocholines	C40H80NO8P	[M+CH3COO]- [M+Na]+	792.5757 756.5535	17.4 17.4	289.8 288.9	2a	0.4 2.8	0.1^{I} 0.9^{I}	↓	↓	↓	↓
PC 32:0		Glycerophosphocholines	C40H80NO8P	[M+H]+	734.5717	17.9	286.3	3	-3.0	0.6^{I}		↓		
PC 32:2	PC 16:1/16:1	Glycerophosphocholines	C40H76NO8P	[M+CH3COO]-	788.5442	15.8	286.5	2a	0.7	2.2^{III}	↓	↓		
PC 34:1		Glycerophosphocholines	C42H82NO8P	[M+Na]+	782.5685	16.4	290.0	3	1.9	-0.7^{I}		↓		
PC 35:1		Glycerophosphocholines	C43H84NO8P	[M+H]+	774.5998	17.9	291.9	3	-1.3	1.2^{II}	↓	↓		
PC 35:2		Glycerophosphocholines	C43H82NO8P	[M+CH3COO]- [M+H]+	830.5909 772.5832	17.4 17.3	295.2 289.8	3	0.9 2.4	2.4^{III} 1.8^{IV}	↓ ↓	↓ ↓		
PC 35:6		Glycerophosphocholines	C43H74NO8P	[M+H]+	764.5225	16.4	278.7	3	0.0	-0.1^{IV}			↓	↓
PC 36:0		Glycerophosphocholines	C44H88NO8P	[M+H]+	790.6340	18.9	297.3	3	-2.4	-0.1^{I}	↓	↓	↓	↓
PC 36:4	PC 16:0_20:4	Glycerophosphocholines	C44H80NO8P	[M+Na]+	804.5516	16.5	290.5	2a	0.2	1.5^{I}		↓		
PC 36:5	PC 16:1_20:4	Glycerophosphocholines	C44H78NO8P	[M+Na]+	802.5344	15.9	287.9	2a	-1.6	0.2^{IV}	↓	↑		
PC 36:5		Glycerophosphocholines	C44H78NO8P	[M+CH3COO]- [M+H]+	838.5595 780.5525	16.2 16.2	293.7 288.0	3	-1.0 -1.6	2.3^{III} 0.9^{II}	↓ ↓	↑ ↑		
PC 36:6		Glycerophosphocholines	C44H76NO8P	[M+Na]+ [M+H]+	800.5214 778.5358	15.2 15.2	285.3 283.9	3	-1.6 3.1	-0.6^{II} -0.1^{II}	↓ ↓	↑ ↑		
PC 37:1		Glycerophosphocholines	C45H88NO8P	[M+H]+	802.6331	18.6	298.3	3	-1.3	0.6^{II}	↓	↓		
PC 37:2		Glycerophosphocholines	C45H86NO8P	[M+H]+	800.6150	18.1	295.7	3	1.7	0.5^{II}	↓	↓		
PC 38:1		Glycerophosphocholines	C46H90NO8P	[M+Na]+ [M+H]+	838.6320 816.6477	18.9 18.9	301.4 298.2	3	2.8 0.0	-0.2^{II} -0.4^{II}	↓ ↓	↓ ↓		
PC 38:2		Glycerophosphocholines	C46H88NO8P	[M+H]+	814.6327	18.4	296.9	3	0.8	0.0^{II}	↓	↓		

Table SI-6.1. Continuation.

Bulk name	Species name	Class	Formula	Ionization species	*m/z*	RT (min)	$^{DT}CCS_{N2}$ (Å^2)	Anno-tation level	Mass error (ppm)	CCS error (%)	IC_{10} exposure		1/10 IC_{10} exposure	
											24h	48h	24h	48h
PC 38:4		Glycerophosphocholines	C46H84NO8P	[M+CH3COO]- [M+H]+	868.6053 810.5999	17.3 17.3	300.8 295.5	3	-2.4 -1.1	2.3[III] 0.5[II]	↓	↓ ↓		
PC 38:6	PC 16:0_22:6	Glycerophosphocholines	C46H80NO8P	[M+Na]+	828.5457	16.5	292.9	2a	6.9	-0.1[II]		↑		
PC 38:6	PC 18:2_20:4	Glycerophosphocholines	C46H80NO8P	[M+Na]+ [M+H]+	828.5496 806.5651	16.1 16.0	292.9 292.4	2a	-2.2 -5.4	-0.1[II] 1.8[IV]	↓	↑ ↑		
PC 40:3		Glycerophosphocholines	C48H90NO8P	[M+H]+	840.6472	18.4	302.9	3	-0.6	0.8[II]	↓	↓		
PC 40:4		Glycerophosphocholines	C48H88NO8P	[M+H]+	838.6299	18.0	301.4	3	2.6	0.4[II]	↓	↓		
PC 40:8		Glycerophosphocholines	C48H80NO8P	[M+H]+	830.5696	15.9	296.3	3	0.1	1.6[II]	↓	↑		
PC O-28:0	PC O-12:0/16:0	Glycerophosphocholines	C36H74NO7P	[M+CH3COO]-	722.5342	16.2	277.8	2a	0.1	2.7[III]	↓	↓		
PC O-30:1		Glycerophosphocholines	C38H76NO7P	[M+H]+	690.5426	16.3	278.5	3	0.8	1.6[IV]	↓	↓		
PC O-30:2		Glycerophosphocholines	C38H74NO7P	[M+H]+	688.5269	15.4	275.1	3	1.0	1.5[IV]	↓	↓		
PC O-32:4		Glycerophosphocholines	C40H74NO7P	[M+H]+	712.5290	15.7	277.7	3	-2.0	2.1[IV]	↓	↓		
PC O-32:5		Glycerophosphocholines	C40H72NO7P	[M+H]+	710.5129	15.1	274.6	3	-1.4	1.4[IV]	↓	↓		
PC O-33:8		Glycerophosphocholines	C41H68NO7P	[M+H]+	718.4804	16.2	277.0	3	-0.2	-0.6[IV]	↓	↓		
PC O-34:5		Glycerophosphocholines	C42H76NO7P	[M+H]+	738.5418	15.4	281.5	3	1.9	2.4[IV]	↓	↓		
PC O-34:7		Glycerophosphocholines	C42H72NO7P	[M+H]+	734.5094	14.9	277.1	3	3.4	1.0[IV]	↓	↓		
PE 32:2	PE 16:1/16:1	Glycerophosphoethano-lamines	C37H70NO8P	[M-H]-	686.4786	16.1	259.0	2a	-2.9	-0.6[II]	↓	↓	↓	↓
PE 34:3	PE 16:1_18:2	Glycerophosphoethano-lamines	C39H72NO8P	[M-H]- [M+H]+	712.4901 714.5063	16.3 16.3	- 269.7	2a	3.1 0.8	- -1.1[IV]	↓ ↓	↓ ↓		
PE 36:2	PE 18:1/18:1	Glycerophosphoethano-lamines	C41H78NO8P	[M+H]+	744.5543	18.0	280.3	2a	0.7	0.4[I]		↓		
PE 36:4	PE 16:0_20:4	Glycerophosphoethano-lamines	C41H74NO8P	[M+H]+	740.5211	17.0	277.1	2a	-1.9	-0.7[IV]				↓
PE 36:5	PE 16:1_20:4	Glycerophosphoethano-lamines	C41H72NO8P	[M+H]+	738.5082	16.4	275.4	2a	1.8	-0.6[IV]	↓			
PE 38:2	PE 18:1_20:1	Glycerophosphoethano-lamines	C43H82NO8P	[M-H]- [M+H]+	770.5689 772.5885	18.7 18.7	278.0 286.4	2a	2.1 -4.4	1.4[II] 0.4[I]	↓ ↓	↓ ↓	↓	↓
PE 38:4	PE 18:1_20:3	Glycerophosphoethano-lamines	C43H78NO8P	[M-H]-	766.5372	17.5	275.5	2a	2.6	-0.1[I]	↓	↓		
PE 38:6	PE 16:0_22:6	Glycerophosphoethano-lamines	C43H74NO8P	[M+H]+	764.5225	16.4	278.7	2a	0.0	-1.0[IV]	↓			
PE 40:2		Glycerophosphoethano-lamines	C45H86NO8P	[M+H]+	800.6156	19.2	293.7	3	1.0	0.6[II]	↓	↓		
PE 40:5		Glycerophosphoethano-lamines	C45H80NO8P	[M+H]+	794.5686	18.7	291.2	3	-1.1	1.4[II]	↓	↓		
PE 40:6	PE 18:1_22:5	Glycerophosphoethano-lamines	C45H78NO8P	[M-H]-	790.5380	17.1	280.7	2a	1.5	0.1[I]	↓	↓		

Table SI-6.1. Continuation.

Bulk name	Species name	Class	Formula	Ionization species	*m/z*	RT (min)	$^{DT}CCS_{N2}$ (Å^2)	Anno-tation level	Mass error (ppm)	CCS error (%)	IC_{10} exposure		1/10 IC_{10} exposure	
											24h	48h	24h	48h
PE O-30:3		Glycerophosphoethano-lamines	C35H66NO7P	[M+H]+	644.4642	15.6	263.1	3	1.2	0.6^{IV}	↓	↓		
PE O-32:5		Glycerophosphoethano-lamines	C37H66NO7P	[M+H]+	668.4628	15.3	263.7	3	3.3	-0.6^{IV}	↓	↓		
PE O-38:4	PE O-18:1/20:3	Glycerophosphoethano-lamines	C43H80NO7P	[M-H]-	752.5587	18.6	276.7	2a	1.6	1.2^{IV}	↓	↓		
PE P-28:0	PE P-16:0/12:0	Glycerophosphoethano-lamines	C33H66NO7P	[M+Na]+	642.4456	16.4	263.2	2a	2.1	0.6^{IV}	↓	↓		
PE P-36:3	PE P-18:1/18:2	Glycerophosphoethano-lamines	C41H76NO7P	[M-H]-	724.5260	17.6	-	2a	3.6	-	↓	↓		
PE P-38:3	PE P-18:0/20:3	Glycerophosphoethano-lamines	C43H80NO7P	[M+H]+	754.5724	18.6	287.2	2a	-2.8	0.7^{IV}	↓	↓		
PEth 34:1	PEth 16:0_18:1	Phosphatidylethanols	C39H75O8P	[M-H]-	701.5110	15.5	264.3	2a	2.5	0.5^{IV}	↑	↑	↑	↑
PG 38:3	PG 18:1_20:2	Glycerophosphoglycer-ols	C44H81O10P	[M-H]-	799.5508	14.8	287.1	2a	-1.7	2.8^{II}	↓	↓		
SM 32:2;2O		Phosphosphingolipids	C37H73N2O6P	[M+H]+	673.5264	14.4	274.6	3	-2.2	1.0^{IV}	↓	↓	↓	↓
SM 33:1;2O		Phosphosphingolipids	C38H77N2O6P	[M+H]+	689.5575	16.1	282.0	3	2.4	1.0^{II}	↓	↓	↓	↓
SM 34:2;2O		Phosphosphingolipids	C39H77N2O6P	[M+CH3COO]- [M+H]+	759.5679 701.5576	15.7 15.7	287.1 282.6	3	-2.8 2.2	2.2^{III} 0.4^{II}	↓ ↓	↓ ↓		
SM 35:2;2O		Phosphosphingolipids	C40H79N2O6P	[M+H]+	715.5743	16.3	-	3	0.8	-	↓	↓		
SM 36:2;2O		Phosphosphingolipids	C41H81N2O6P	[M+H]+	729.5909	16.7	289.0	3	0.6	1.3^{I}	↓	↓		
SM 38:0;2O		Phosphosphingolipids	C43H89N2O6P	[M+H]+	761.6509	18.6	-	3	2.9	-			↓	
SM 38:2;2O		Phosphosphingolipids	C43H85N2O6P	[M+H]+	757.6220	17.6	294.6	3	0.3	1.3^{IV}	↓	↓		
SM 40:2;2O		Phosphosphingolipids	C45H89N2O6P	[M+H]+	785.6537	18.4	300.2	3	-0.8	1.1^{I}	↓	↓		
SM 41:2;2O		Phosphosphingolipids	C46H91N2O6P	[M+H]+	799.6710	18.7	302.3	3	-2.8	0.7^{I}	↓	↓	↓	↓
SM 41:3;2O		Phosphosphingolipids	C46H89N2O6P	[M+H]+	797.6578	18.0	-	3	-5.9	-	↓		↓	
SM 43:1;2O		Phosphosphingolipids	C48H97N2O6P	[M+H]+	829.7136	19.8	310.2	3	2.5	0.7^{I}	↓	↓		
TG 50:4	TG 16:1_16:1_18:2	Triradylglycerols	C53H94O6	[M+NH4]+	844.7380	21.1	310.3	2a	1.0	-0.9^{II}		↑		
TG 52:5	TG 16:1_18:2_18:2	Triradylglycerols	C55H96O6	[M+NH4]+	870.7567	21.1	314.7	2a	-2.5	1.6^{II}		↑		
TG 54:6	TG 16:1_18:1_20:4	Triradylglycerols	C57H98O6	[M+NH4]+	896.7717	21.3	318.2	2a	-1.8	-1.2^{II}	↑	↑		
TG O-46:1	TG O-17:0_11:0_18:1	Triradylglycerols	C49H94O5	[M+NH4]+	780.7461	21.8	302.3	2a	2.8	-0.1^{IV}	↑	↑		
TG P-48:1	TG P-16:1_16:0_16:0	Triradylglycerols	C51H96O5	[M+NH4]+	806.7573	21.8	305.9	2a	-2.9	-1.2^{IV}	↑	↑		

Section 7. Metabolic changes in the extracellular fraction of HepaRG cells

Table SI-7.1. Annotated metabolites that showed alterations after ethanol exposure in the extracellular fraction of HepaRG cells. Classes were adopted from LIPID MAPS for lipids and from HMDB for polar metabolites. CCS errors were calculated comparing obtained experimental single-field $^{DT}CCS_{N2}$ with experimental database values from CCS compendium ([I]), CCSbase ([II]), MS-DIAL internal lipidomic library v. 4.6 ([III]) or *in silico* generated CCS values using AllCCS ([IV]).[4–7] Annotation levels refer to the confidence levels of Schymanski et al.[8]

Bulk name	Species name	Class	Formula	Ionization species	*m/z*	RT (min)	$^{DT}CCS_{N2}$ (Å^2)	Annotation level	Mass error (ppm)	CCS error (%)	IC_{10} exposure		1/10 IC_{10} exposure	
											24h	48h	24h	48h
Ethoxylated phosphorylcholine	2-[Ethoxy(hydroxy)phosphoryl]oxyethyl-trimethylazanium	Organonitrogen compounds	C7H19NO4P+	[M]+	212.1049	13.5	-	2b	-1.4	-	↑	↑	↑	↑
20-dihydrocortisol	20-dihydrocortisol	Steroids	C21H32O5	[M+H]+	365.2333	1.9	-	2a	2.8	-	↓	↓	↓	↓
4-pyridoxic acid	4-pyridoxic acid	Pyridines and derivatives	C8H9NO4	[M-H]-	182.0457	1.5	-	2a	-1.2	-		↓		
Alanylglutamine	Alanylglutamine	Carboxylic acids and derivatives	C8H15N3O4	[M+H]+	218.1139	13.9	-	2a	1.5	-	↓	↓		
Beta-alanine	Beta-alanine	Carboxylic acids and derivatives	C3H7NO2	[M+H]+	90.0550	7.6	-	2a	0.5	-			↓	↓
Glycerophosphocholine	Glycerophosphocholine	Glycerophosphocholines	C8H20NO6P	[M+H]+	258.1102	14.2	-	2a	0.5	-	↑	↑		
Histidylleucine	Histidylleucine	Carboxylic acids and derivatives	C12H20N4O3	[M+H]+	269.1616	14.0	-	2a	3.1	-	↓	↓		
Hypoxanthine	Hypoxanthine	Imidazopyrimidines	C5H4N4O	[M+H]+	137.0459	8.8	-	1	0.9	-	↑	↑		
Inosine	Inosine	Purine nucleosides	C10H12N4O5	[M+H]+	269.0894	8.8	-	1	4.9	-	↑	↑		
N-acetyl-lactosamine	N-acetyl-lactosamine	Organooxygen compounds	C14H25NO11	[M+Na]+	406.1336	10.8	-	2a	3.9	-	↓	↓		
Phenylacetylglutamine	Phenylacetylglutamine	Carboxylic acids and derivatives	C13H16N2O4	[M+H]+	265.1179	8.3	-	1	-1.4	-	↓	↓		
Phosphorylcholine	Phosphorylcholine	Organonitrogen compounds	C5H15NO4P+	[M]+	184.0734	14.9	-	1	-2.7	-	↑	↑		
Cer 34:1;2O	Cer 18:1;O2/16:0	Ceramides	C34H67NO3	[M+CH3COO]-	596.5236	17.7	254.6	1	-3.9	0.6[III]	↑	↑		
LPC 16:1	LPC 16:1	Glycerophosphocholines	C24H48NO7P	[M+CH3COO]-	552.3290	8.1	238.2	2a	-3.0	2.6[III]	↓	↓		
LPC 17:0	LPC 17:0	Glycerophosphocholines	C25H52NO7P	[M+H]+ [M+Na]+	510.3548 532.3369	9.6 9.6	233.3 235.5	2a	-1.1 -0.8	-0.4[II] -0.9[II]	↓ ↓	↓ ↓		
LPC 18:0	LPC 18:0	Glycerophosphocholines	C26H54NO7P	[M+H]+ [M+Na]+	524.3690 546.3536	10.5 10.4	237.9 239.2	2a	-4.0 1.1	-0.4[I] -1.0[I]	↓ ↓	↓ ↓		
LPC 18:1	LPC 18:1	Glycerophosphocholines	C26H52NO7P	[M+H]+	522.3551	9.1	234.6	2a	-0.5	0.6[I]	↓	↓		
LPC 20:1	LPC 20:1	Glycerophosphocholines	C28H56NO7P	[M+Na]+	572.3681	10.6	243.3	2a	-0.9	0.2[II]	↓	↓		

Table SI-7.1. Continuation.

Bulk name	Species name	Class	Formula	Ionization species	*m/z*	RT (min)	$^{DT}CCS_{N2}$ (Å^2)	Anno-tation level	Mass error (ppm)	CCS error (%)	IC_{10} exposure		1/10 IC_{10} exposure	
											24h	48h	24h	48h
LPC P-16:0	LPC P-16:0	Glycerophosphocho-lines	C24H50NO6P	[M+Na]+	502.3267	9.4	227.4	2a	-0.2	-1.7[IV]	↓	↓		
PE 32:1	PE 16:0_16:1	Glycerophosphoethano-lamines	C37H72NO8P	[M-H]-	688.4900	17.0	260.6	2a	-3.4	1.5[II]			↑	↑
PE 36:1	PE 18:0_18:1	Glycerophosphoethano-lamines	C41H80NO8P	[M-H]-	744.5538	18.4	271.8	2a	-1.5	-0.6[I]	↑	↑	↑	↑
PE 36:4	PE 16:0_20:4	Glycerophosphoethano-lamines	C41H74NO8P	[M+H]+	740.5198	17.1	276.6	2a	-3.6	1.6[II]	↑	↑		
PE 38:4	PE 18:0_20:4	Glycerophosphoethano-lamines	C43H78NO8P	[M-H]- [M+H]+	766.5367 768.5520	17.8 17.9	274.5 284.3	2a	-3.3 -2.3	-0.5[I] 0.3[II]	↑ ↑	↑ ↑		

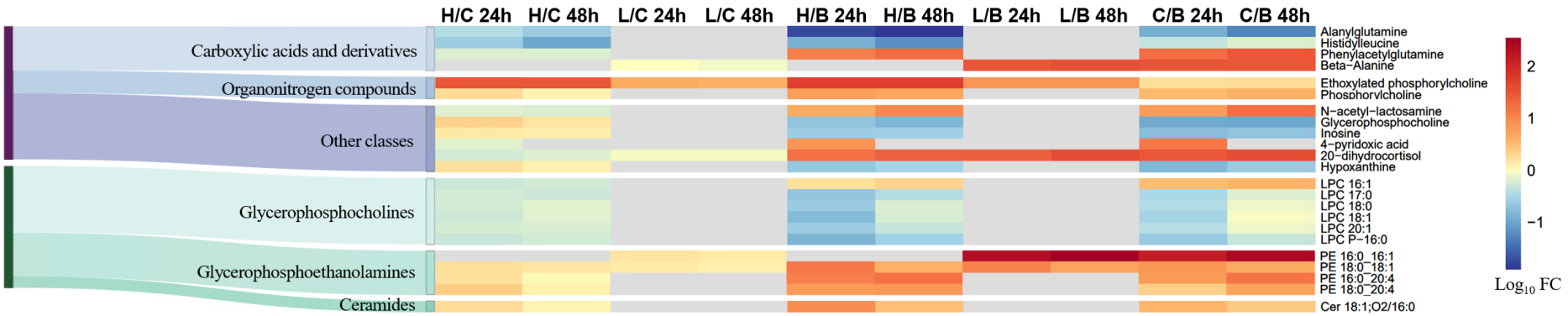

Fig. SI-7.1. Sankey diagram combined with heatmaps to show the effect of ethanol exposure on the extracellular metabolome of HepaRG cells. Only annotated metabolites which were selected by univariate and/or multivariate statistics are shown. Altered metabolites in the polar fraction of the samples are indicated by a blue-purple Sankey diagram, while a green Sankey diagram represents metabolites originating from the apolar fraction. Grey color in the heatmap was used when a metabolite was not selected during the statistical selection. H/C 24 h: IC_{10} vs. control after 24 h of ethanol exposure. H/C 48 h: IC_{10} vs control after 48 h of ethanol exposure. L/C 24 h: 1/10 IC_{10} vs control after 24 h of ethanol exposure. L/C 48 h: 1/10 IC_{10} vs control after 48 h of ethanol exposure. H/B 24 h: IC_{10} vs blank media after 24 h of ethanol exposure. H/B 48 h: IC_{10} vs blank media after 48 h of ethanol exposure. L/B 24 h: 1/10 IC_{10} vs blank media after 24 h of ethanol exposure. L/B 48 h: 1/10 IC_{10} vs blank media after 48 h of ethanol exposure. C/B 24 h: Control vs blank media after 24 h of incubation. C/B 48 h: Control vs blank media after 48 h of incubation. FC: fold change.

Section 8. Examples of MS/MS spectra

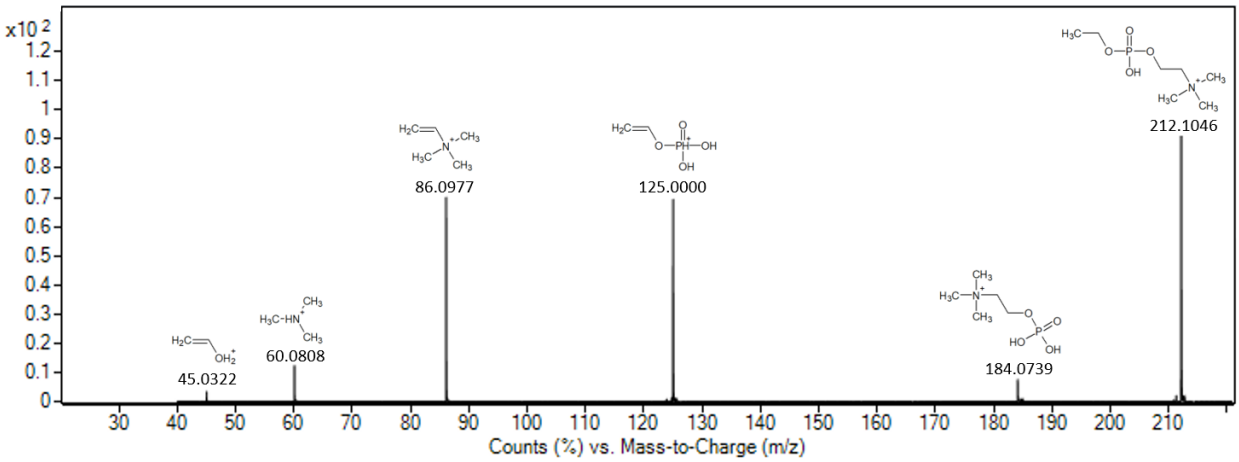

Fig. SI-8.1. MS/MS spectrum of ethoxylated phosphorylcholine at 10 eV after maximum intensity normalization. The spectrum was measured in the extracellular polar fraction of HepaRG cells (ESI (+)). Fragment structures were derived from CFM-ID.

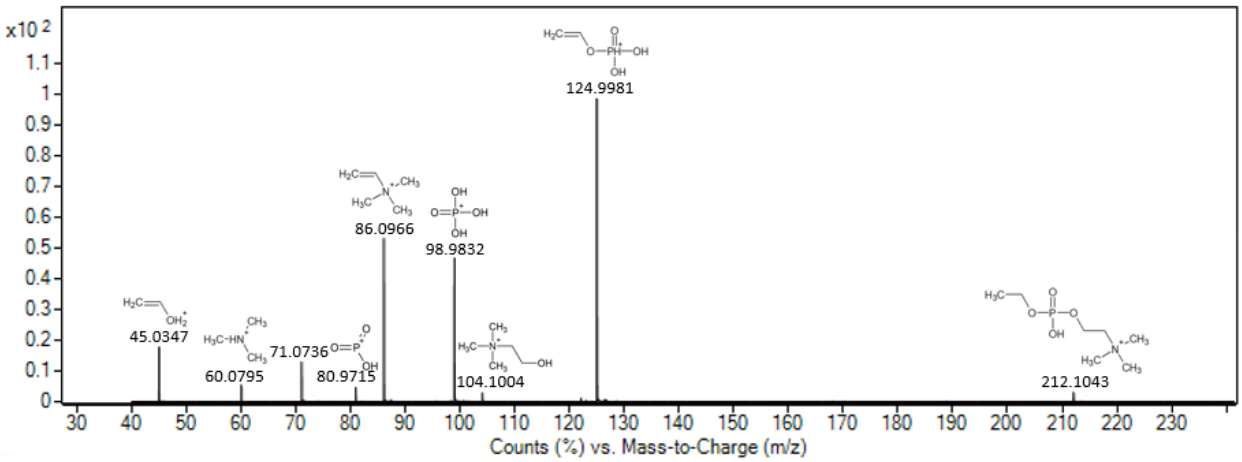

Fig. SI-8.2. MS/MS spectrum of ethoxylated phosphorylcholine at 20 eV after maximum intensity normalization. The spectrum was measured in the extracellular polar fraction of HepaRG cells (ESI (+)). Fragment structures were derived from CFM-ID.

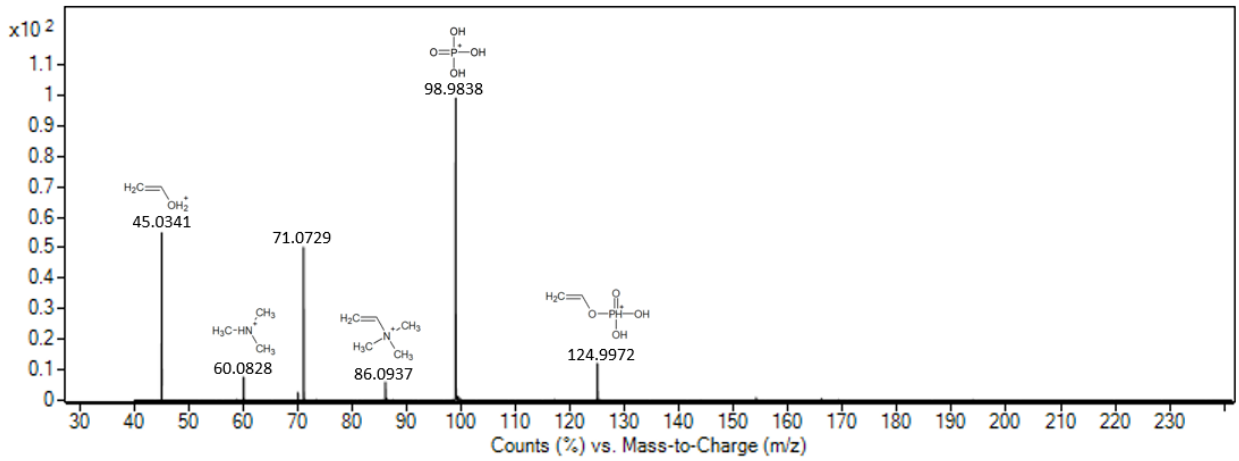

Fig. SI-8.3. MS/MS spectrum of ethoxylated phosphorylcholine at 40 eV after maximum intensity normalization. The spectrum was measured in the extracellular polar fraction of HepaRG cells (ESI (+)). Fragment structures were derived from CFM-ID.

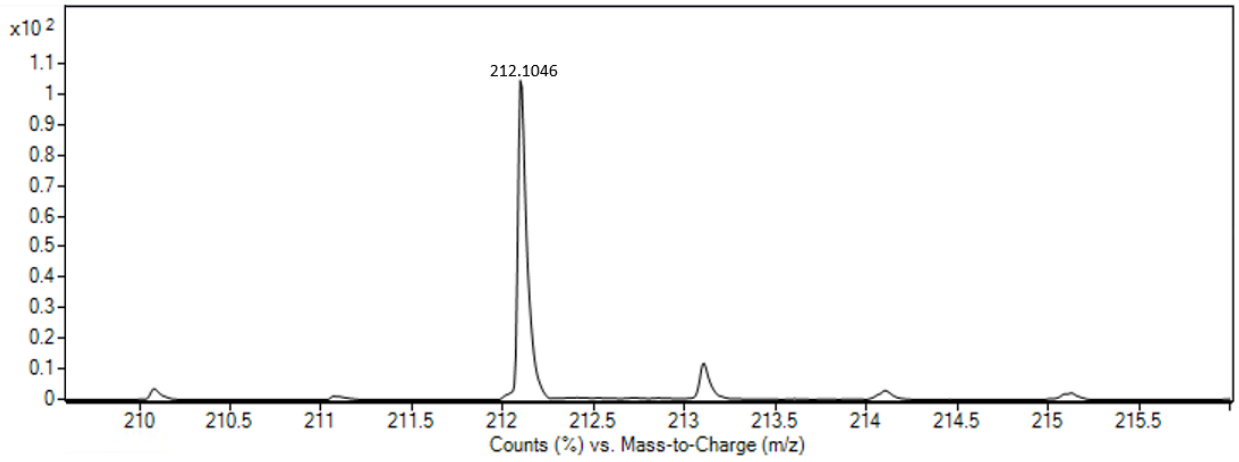

Fig. SI-8.4. Isotopic pattern of ethoxylated phosphorylcholine. The spectrum was measured in the extracellular polar fraction of HepaRG cells (ESI (+)).

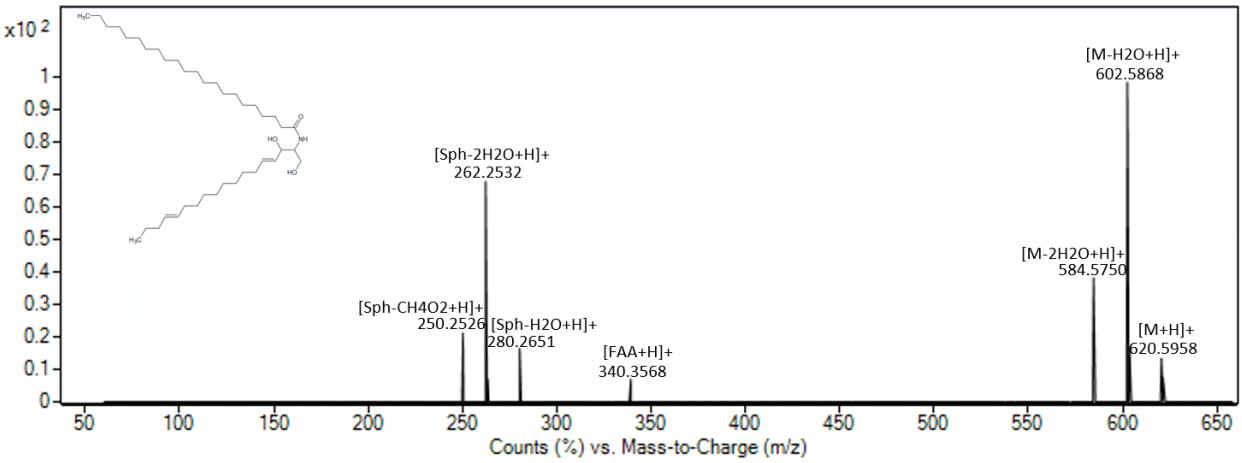

Fig. SI-8.5. MS/MS spectrum of Cer 18:2;O2/22:0 at 10 eV after maximum intensity normalization. The spectrum was measured in the intracellular apolar fraction of HepaRG cells (ESI (+)). Fragment structures are not shown due to their size. FAA: fatty acid ammonia (i.e., FA-OH+NH3). Sph: Sphingoid base.

REFERENCES

(1) Cuykx, M.; Mortelé, O.; Rodrigues, R. M.; Vanhaecke, T.; Covaci, A. Optimisation of: In Vitro Sample Preparation for LC-MS Metabolomics Applications on HepaRG Cell Cultures. *Anal. Methods* **2017**, *9* (24), 3704–3712. https://doi.org/10.1039/c7ay00573c.

(2) Dettmer, K.; Vogl, F. C.; Ritter, A. P.; Zhu, W.; Nürnberger, N.; Kreutz, M.; Oefner, P. J.; Gronwald, W.; Gottfried, E. Distinct Metabolic Differences between Various Human Cancer and Primary Cells. *Electrophoresis* **2013**, *34* (19), 2836–2847. https://doi.org/10.1002/elps.201300228.

(3) Wu, Z. E.; Kruger, M. C.; Cooper, G. J. S.; Poppitt, S. D.; Fraser, K. Tissue-Specific Sample Dilution: An Important Parameter to Optimise Prior to Untargeted LC-MS Metabolomics. *Metabolites* **2019**, *9* (7), 1–19. https://doi.org/10.3390/metabo9070124.

(4) Picache, J. A.; Rose, B. S.; Balinski, A.; Leaptrot, K. L.; Sherrod, S. D.; May, J. C.; McLean, J. A. Collision Cross Section Compendium to Annotate and Predict Multi-Omic Compound Identities. *Chem. Sci.* **2019**, *10* (4), 983–993. https://doi.org/10.1039/c8sc04396e.

(5) Ross, D. H.; Cho, J. H.; Xu, L. Breaking Down Structural Diversity for Comprehensive Prediction of Ion-Neutral Collision Cross Sections. *Anal. Chem.* **2020**, *92* (6), 4548–4557. https://doi.org/10.1021/ACS.ANALCHEM.9B05772.

(6) Tsugawa, H.; Ikeda, K.; Takahashi, M.; Satoh, A.; Mori, Y.; Uchino, H.; Okahashi, N.; Yamada, Y.; Tada, I.; Bonini, P.; Higashi, Y.; Okazaki, Y.; Zhou, Z.; Zhu, Z.-J.; Koelmel, J.; Cajka, T.; Fiehn, O.; Saito, K.; Arita, M.; Arita, M. A Lipidome Atlas in MS-DIAL 4. *Nat. Biotechnol.* **2020**, *38* (10), 1159–1163. https://doi.org/10.1038/s41587-020-0531-2.

(7) Zhou, Z.; Luo, M.; Chen, X.; Yin, Y.; Xiong, X.; Wang, R.; Zhu, Z. J. Ion Mobility Collision Cross-Section Atlas for Known and Unknown Metabolite Annotation in Untargeted Metabolomics. *Nat. Commun.* **2020**, *11* (1), 1–13. https://doi.org/10.1038/s41467-020-18171-8.

(8) Schymanski, E. L.; Jeon, J.; Gulde, R.; Fenner, K.; Ruff, M.; Singer, H. P.; Hollender, J. Identifying Small Molecules via High Resolution Mass Spectrometry: Communicating Confidence. *Environ. Sci. Technol.* **2014**, *48* (4), 2097–2098. https://doi.org/10.1021/ES5002105.